ELSEVIER

Journal of Alloys and Compounds 323–324 (2001) 811–815

Journal of ALLOYS AND COMPOUNDS

www.elsevier.com/locate/jallcom

# Simulation of the $Gd^{3+}$ energy level scheme in GdOCl

Jorma Hölsä[a,c], Ralf-Johan Lamminmäki[a,b,1], Mika Lastusaari[a,b,*], Pierre Porcher[c]

[a]*Department of Chemistry, University of Turku, FIN-20014 Turku, Finland*
[b]*Graduate School of Materials Research, Turku, Finland*
[c]*Laboratoire de Chimie Appliquée de l'Etat Solide, UMR 7574 CNRS, ENSCP, F-75231 Paris Cedex 05, France*

## Abstract

The luminescence materials of the new generation containing gadolinium have received considerable attention because of the quantum cutting and down-conversion exhibited. The prerequisite information for studies of these phenomena include a detailed analysis of the UV energy level scheme of the $Gd^{3+}$ ion with the $4f^7$ electron configuration. In this paper such a study was carried out for the tetragonal GdOCl matrix. The UV absorption spectra of GdOCl were measured at 9 K between 200 and 315 nm. The experimental energy level scheme derived from the spectra was interpreted according to the $C_{4v}$ site symmetry of the $Gd^{3+}$ site in the oxychloride matrix. This level scheme of 24 c.f. components representing seven $^{2S+1}L_J$ ($^8S_{7/2}$, $^6P_J$, $^6I_J$, $^6D_J$) levels was then successfully simulated by a phenomenological model using 14 free ion and five real c.f. parameters. A satisfactory match with an rms deviation of 21 $cm^{-1}$ between the experimental and calculated energy level schemes was obtained despite the high number of parameters and the sparse set of energy levels. The present results obtained for GdOCl were found consistent with the previous ones for other $RE^{3+}$ ions in the REOCl hosts.

*Keywords:* Phosphors; Crystal and ligand fields; Electronic states; Optical properties; Light absorption

## 1. Introduction

Due to environmental reasons, a need has arisen to replace with (a) new UV emitting substance(s) the mercury supplying the exciting UV radiation to the phosphors in tricolour fluorescence tubes. The few materials suggested to replace mercury include the noble gases which emit UV radiation that does not match the absorption of the present phosphors and thus new phosphors will be needed, too. The development of new phosphors and, in general, applications based on the luminescence of the trivalent rare earth ions ($RE^{3+}$) requires the exact knowledge of their $4f^N$ energy level schemes. In the new fluorescence lamps the minimization of the loss of excitation energy is even more important due to the high energy of the UV radiation emitted by the noble gases. One solution to this is to convert one quantum of the exciting UV-radiation into two quanta of visible light [1]. This may yield quantum efficiencies higher than 100% because of the high luminescence efficiency of the trivalent rare earth ions, though the excitation energy lost in the non-radiative de-excitation processes in the VUV and UV ranges may be prohibitively high.

The quantum cutting can be achieved with the presence of several $RE^{3+}$ ions in a matrix containing a high amount of the $Gd^{3+}$ ion. Such phenomena have been observed with the activator(–co-activator) systems of $Er^{3+}$, $Tb^{3+}$ [2,3], and $Eu^{3+}$ [3,4] in the $LiYF_4$ host matrix. Although the energy level scheme of the (co-)activator finally determines the emission properties of the phosphor — such as the emission color, for example, the knowledge of the level scheme of the $Gd^{3+}$ ion is equally important since transfer of the excitation energy between different $RE^{3+}$ ion is involved in the quantum cutting process. Studies of the energy level scheme of the $Gd^{3+}$ ion are still very infrequent, although the determination of the famous Dieke's diagram [5] dates already from three decades. The validity of the famous Dieke's diagram is, however, restricted mainly to energies below the UV threshold. Only quite recently the UV part of the energy level schemes of the $RE^{3+}$ ions has become accessible with the aid of a combination of synchrotron radiation and theoretical calculations [6].

The $Gd^{3+}$ ion has the $4f^7$ electron configuration which has the most complicated energy level scheme in the whole

---

*Corresponding author. Tel.: +358-2-333-6736; fax: +358-2-333-6700.

*E-mail address:* miklas@utu.fi (M. Lastusaari).

[1] Present address: Kemira Pigments Ltd., FIN-28840 Pori, Finland.

0925-8388/01/$ – see front matter
PII: S0925-8388(01)01150-1

$RE^{3+}$ series. The energy level scheme of the $Gd^{3+}$ ion consists of 327 free ion spin–orbit coupled $^{2S+1}L_J$ levels which can split into up to 3432 c.f. levels for a $RE^{3+}$ site with lower than cubic symmetry [7]. In fact, the number of Stark levels to be observed is much less since in the absence of an external magnetic field the 3432 levels occur as 1716 Kramers doublets. The high degeneracy of the $4f^7$ electron configuration is not the only reason for the very few studies dealing with the determination of the energy level structure of the $Gd^{3+}$ ion: a wide energy gap of ca 32 000 $cm^{-1}$ exists between the $^8S_{7/2}$ ground level and the first excited term, $^6P_J$. The number of levels accessible by one-photon absorption experiments before the threshold of the VUV region, the lattice absorption or the absorption to the $4f^65d^1$ electron configuration is thus very limited. The limitations on the theoretically accessible levels can partially be lifted by the application of two-photon absorption techniques but only combined with the rather cumbersome vacuum setups required for the VUV region. Finally, at even higher energies, the density of the 4f levels is rather high making the identification and labeling of the energy levels difficult if not impossible.

The investigations of the energy level structure of the $Gd^{3+}$ ion have mainly been restricted to the halide lattices ($LaF_3$ [8], $CaF_2$ [9], $LaCl_3$ [10], and $Cs_2NaGdCl_6$ [11]) although the oxidic ($RE(OH)_3$ [12], $Y(OH)_3$ [12], $RE(C_2H_5SO_4)_3\cdot 9H_2O$ (RES) [13], $Na_3[RE(C_4H_4O_5)_3]\cdot 2NaClO_4\cdot 6H_2O$ (RODA) [14]) have been considered, too. The investigations dealing with the $Gd^{3+}$ ion are very few, indeed. The preference to study the host lattices containing fluorine can be explained as follows: in fluorides the absorption by the $4f^65d^1$ electron configuration should be shifted to the maximum energy. The energy of the $4f^65d^1$ configuration of the $Gd^{3+}$ ion in $CaF_2$ host approaches 80 000 $cm^{-1}$ [15,16], which is the highest among the $RE^{3+}$ ions matching even $Lu^{3+}$, though probably not $La^{3+}$. This fact allows the very interesting but also the very complicated studies of the high energy level schemes of the $RE^{3+}$ ions.

The tetragonal RE oxychlorides (REOCl) are known as efficient phosphors and may be potential candidates for the luminescent materials of the new generation. On the other hand, this host matrix offers an excellent possibility for use as a model system for spectroscopic studies because of the relatively high ($C_{4v}$) point symmetry of the $RE^{3+}$ site. The layered, practically two-dimensional structure induces detailed investigations of interesting energy transfer phenomena, too.

In this work, the systematic study of the $4f^7$ electron configuration of the $Gd^{3+}$ ion in GdOCl was carried out by measuring the UV-absorption spectra of GdOCl (and GdOCl:$RE^{3+}$) at 9 K. The experimental crystal field (c.f.) level scheme thus obtained was simulated with a phenomenological model accounting simultaneously for the free ion and c.f. interactions. The GdOCl parameter set was compared with those of the $Pr^{3+}$ [17], $Nd^{3+}$ [18], $Sm^{3+}$ (Hölsä, J., Lamminmäki, R.-J., Porcher, P., 1998, unpublished data), $Eu^{3+}$ [19], $Tb^{3+}$ [20], $Dy^{3+}$ [21], $Ho^{3+}$ [22], $Er^{3+}$ [23] and $Tm^{3+}$ [24] ions in REOCl hosts.

## 2. Experimental

The polycrystalline GdOCl (and GdOCl:$RE^{3+}$; $RE^{3+}$ = $Er^{3+}$, $Ho^{3+}$, and $Tm^{3+}$; $x_{RE} = 0.09$) samples were prepared by the solid state reaction between $RE_2O_3$ and $NH_4Cl$ ($NH_4Cl/RE_2O_3$ ratio equal to 2.1) at 900°C for 1.5 h [25]. The purity of the products was verified by routine X-ray powder diffraction analysis but no impurities were found.

The lighter RE oxychlorides (RE = La–Er, and Y) crystallise in the tetragonal Matlockite-type PbFCl structure with *P4/nmm* (#129; $Z=2$) as the space group [26]. The crystal structure of GdOCl comprises of alternating layers of the $(REO)_n^{n+}$ complex cations and the $Cl^-$ anions typical of the tetragonal RE oxycompounds [27]. The $Gd^{3+}$ cation is coordinated to four oxygens and five chlorines in a monocapped square antiprism arrangement with $C_{4v}$ as the point symmetry of the $Gd^{3+}$ site.

The UV absorption spectra of GdOCl were obtained with a Varian Cary 5E apparatus in the 200–315 nm range at 9 K with a reproducibility better than 0.04 Å. The low temperature reduces the broadening and possible superimposition of adjacent absorption lines. Measurements at higher temperatures are not necessary since no hot band absorption yielding additional spectral information can be achieved due to the very small c.f. splitting of the $^8S_{7/2}$ ground level (of the order of 1 $cm^{-1}$). The absorption of the GdOCl:$RE^{3+}$ co-doped samples was found stronger than the pure GdOCl possibly due to the co-operative effects. The energy level schemes of the $Gd^{3+}$ ion obtained from the interpretation of the spectra of the co-doped samples were, however, not used since the level energies were varied slightly from one GdOCl:$RE^{3+}$ system to another because of the presence of the $RE^{3+}$ co-dopant. Moreover, the absorption of the $RE^{3+}$ ions was sometimes superimposed with the proper absorption lines of the $Gd^{3+}$ ion.

## 3. Results and discussion

### 3.1. Absorption spectra

The absorption spectrum of the $Gd^{3+}$ ion in GdOCl shows no sharp lines typical for the $RE^{3+}$ ions in the visible range but is composed of groups of lines in the UV range only (Fig. 1). Despite the high degeneracy of the $4f^7$ configuration the density of levels in the lower part of the UV region is rather low which results in only a few

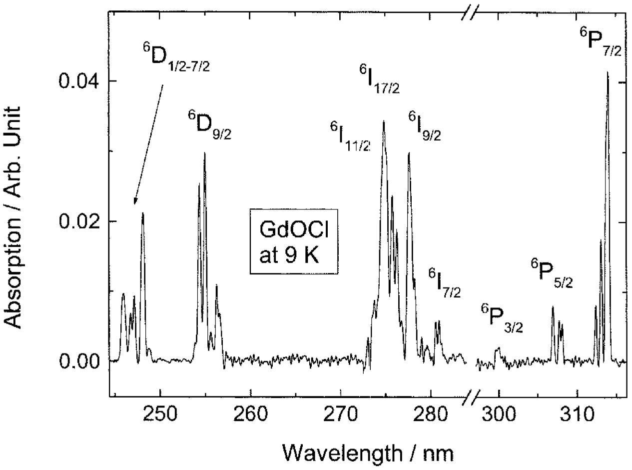

Fig. 1. Parts of the absorption spectrum of GdOCl at 9 K.

isolated groups lines originating from the transitions from the $^8S_{7/2}$ ground level. Since the splitting of the $^8S_{7/2}$ level is very small and beyond the resolution of the apparatus used all the transitions to excited Stark levels occur as single lines and are directly connected to the crystal field components of the excited $^{2S+1}L_J$ levels.

In the UV region, the first levels observed by one-photon absorption were $^6P_{7/2}$ and $^6P_{5/2}$, for which all seven c.f. Stark levels were observed between 307 and 314 nm. Absorption to the c.f. levels of the next term, $^6I$, is very weak and only a few scattered c.f. levels could be extracted from the spectra. The absorption to the next — and the last to be observed (Fig. 2) — term, $^6D$, is much stronger. The c.f. splitting of the free ion levels is very weak — for example the total splitting between the four c.f. levels of the $^6P_{7/2}$ level is only 160 $cm^{-1}$ — which leads to a severe superimposition of the absorption lines. Eventually, due to the weak absorption strength and to the consequent relatively weak resolution only a total of 24 c.f. Stark levels out of 64 were obtained from the careful analysis of the $^8S_{7/2} \rightarrow {}^6P_{3/2-7/2}$, $^8S_{7/2} \rightarrow {}^6I_{7/2-17/2}$ and $^8S_{7/2} \rightarrow {}^6D_{1/2-9/2}$ transitions in the absorption spectra of the $Gd^{3+}$ ion in GdOCl (Table 1).

The number of the Stark levels (Kramers doublets) for a free ion $^{2S+1}L_J$ ($J$ = non-integer) state is $J+1/2$ for any symmetry lower than cubic [28]. The 1716 c.f. Stark levels of the $Gd^{3+}$ ion are labeled as either $D_{1/2}$ or $_2S$. According to the group theoretical selection rules, transitions between all Stark levels are allowed as both electric (e.d) and magnetic (m.d.) dipole transitions. The transitions from the $^8S_{7/2}$ ground level arise mainly due to the e.d. interaction with the $\Delta J \leq 6$ selection rule [29] because of the rather high $J$ value of the ground level. No exclusion of transitions between the Stark levels occurs in the wave length region studied. The selection rule $\Delta J = 0, \pm 1$ [29] restricts the number of possible m.d. transitions but their existence cannot be excluded, either. Although the free ion selection rules can be considered to be broken down in a crystalline matter it is evident from the absorption spectrum of the $Gd^{3+}$ ion in GdOCl (Fig. 1) that even the free ion selection rules involving the orbital quantum number $L$ have a visible effect on the strength of the absorption lines.

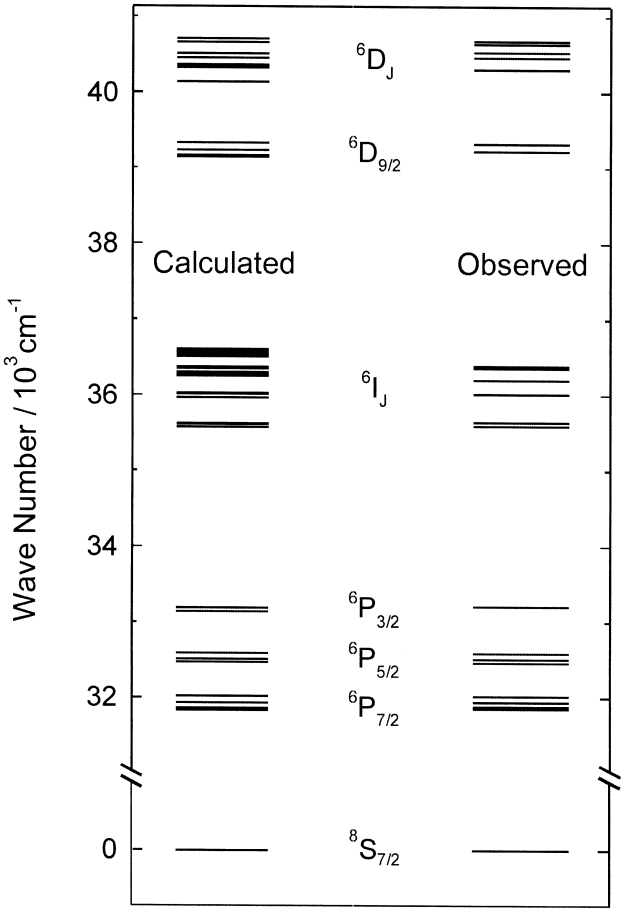

Fig. 2. Energy level scheme of the $Gd^{3+}$ ion in GdOCl.

### 3.2. Energy Level Scheme Simulation

The simulation of the energy level scheme of the $4f^7$ configuration was carried out by using a phenomenological model which treated simultaneously both the free ion and c.f. effects despite the high degeneracy of the electron configuration. Furthermore, no truncation of the set of the basis functions was used. The Hamiltonian, $H_{TOT}$, used in this work (Eqs. (1) and (2)) includes one or several parameters for each interaction [7,29,30]. The effective free ion Hamiltonian included the Slater integrals, $F^k$ ($k$ = 0,2,4,6) accounting for the Coulombic repulsion between the 4f electrons, $\zeta_{4f}$ representing the spin–orbit interaction as well as the Trees ($\alpha,\beta,\gamma$) and Judd ($T^k$; $k$ = 2,3,4,6,7,8) parameters describing the two- and three-body configuration interactions, respectively [29,30].

Table 1
Calculated and experimental energy level schemes in GdOCl (in $\mathrm{cm}^{-1}$)

| Level | | $E_{\mathrm{calc}}$ | $E_{\mathrm{obs}}$ |
|---|---|---|---|
| $^8S_{7/2}$ | $D_{1/2}$ | −1 | 0 |
| | $_2S$ | 0 | 0 |
| | $_2S$ | 0 | 0 |
| | $D_{1/2}$ | 1 | 0 |
| $^6P_{7/2}$ | $D_{1/2}$ | 31 822 | 31 851 |
| | $_2S$ | 31 853 | 31 876 |
| | $_2S$ | 31 926 | 31 943 |
| | $D_{1/2}$ | 32 010 | 32 016 |
| $^6P_{5/2}$ | $D_{1/2}$ | 32 466 | 32 463 |
| | $_2S$ | 32 505 | 32 506 |
| | $_2S$ | 32 591 | 32 584 |
| $^6P_{3/2}$ | $_2S$ | 33 135 | |
| | $D_{1/2}$ | 33 191 | |
| $^6I_{7/2}$ | $_2S$ | 35 567 | 35 595 |
| | $D_{1/2}$ | 35 573 | |
| | $D_{1/2}$ | 35 610 | |
| | $_2S$ | 35 613 | 35 640 |
| $^6I_{9/2}$ | $_2S$ | 35 966 | |
| | $D_{1/2}$ | 35 966 | |
| | $_2S$ | 36 015 | |
| | $D_{1/2}$ | 36 019 | 36 031 |
| | $D_{1/2}$ | 36 025 | |
| $^6I_{17/2}$ | $D_{1/2}$ | 36 248 | 36 200 |
| | $_2S$ | 36 249 | |
| | $D_{1/2}$ | 36 253 | |
| | $_2S$ | 36 254 | |
| | $_2S$ | 36 259 | |
| | $D_{1/2}$ | 36 262 | |
| | $D_{1/2}$ | 36 265 | |
| | $_2S$ | 36 272 | 36 258 |
| | $D_{1/2}$ | 36 272 | 36 258 |
| $^6I_{11/2}$ | $D_{1/2}$ | 36 299 | |
| | $_2S$ | 36 300 | |
| | $_2S$ | 36 344 | |
| | $D_{1/2}$ | 36 354 | |
| | $_2S$ | 36 358 | 36 385 |
| | $D_{1/2}$ | 36 367 | |
| $^6I_{13/2}$ | $_2S$ | 36 502 | |
| | $D_{1/2}$ | 36 505 | |
| $^6I_{15/2}$ | $_2S$ | 36 525 | |
| | $D_{1/2}$ | 36 532 | |
| $^6I_{13/2}$ | $_2S$ | 36 556 | |
| | $D_{1/2}$ | 36 558 | |
| $^6I_{15/2}$ | $D_{1/2}$ | 36 563 | |
| $^6I_{13/2}$ | $_2S$ | 36 564 | |
| $^6I_{15/2}$ | $_2S$ | 36 571 | |
| | $D_{1/2}$ | 36 571 | |
| | $_2S$ | 36 575 | |
| | $D_{1/2}$ | 36 582 | |
| | $D_{1/2}$ | 36 590 | |
| | $_2S$ | 36 593 | |
| | $_2S$ | 36 600 | |
| $^6D_{9/2}$ | $_2S$ | 39 146 | 39 136 |
| | $D_{1/2}$ | 39 158 | |
| | $_2S$ | 39 234 | 39 228 |
| | $D_{1/2}$ | 39 235 | |
| | $D_{1/2}$ | 39 329 | 39 324 |
| $^6D_{1/2}$ | $D_{1/2}$ | 40 142 | |
| $^6D_{7/2}$ | $D_{1/2}$ | 40 326 | 40 310 |
| | $_2S$ | 40 350 | |
| | $D_{1/2}$ | 40 356 | |
| | $_2S$ | 40 368 | |
| $^6D_{3/2}$ | $D_{1/2}$ | 40 456 | 40 463 |
| | $_2S$ | 40 515 | 40 535 |
| $^6D_{5/2}$ | $_2S$ | 40 658 | |
| | $D_{1/2}$ | 40 660 | 40 677 |
| | $_2S$ | 40 712 | |

$$H = \sum_{k=0,2,4,6} F^k(nf, nf) f_k + \zeta_{4f} A_{\mathrm{SO}} + \alpha L(L+1) + \beta(G_2) + \gamma G(R_7) + \sum_{k=2,3,4,6,7,8} T^k t_k \tag{1}$$

The c.f. part of the Hamiltonian was represented by the $B_q^k$ (and $S_q^k$) c.f. parameters, the number of which is defined by the site symmetry of the $\mathrm{RE}^{3+}$ ion [28]. For the rather high $C_{4v}$ symmetry of the $\mathrm{Gd}^{3+}$ site in GdOCl, the number of the non-zero c.f. parameters is restricted to five real ones, i.e., $B_0^2$, $B_0^4$, $B_4^4$, $B_0^6$, and $B_4^6$. All the imaginary parts $S_q^k$ are thus zero.

$$H_{\mathrm{CF}} = \sum_k \sum_{q=0}^{k} \{B_q^k [C_q^k + (-1)^q C_{-q}^k] + i S_q^k [C_q^k - (-1)^{-q} C_{-q}^k]\} \tag{2}$$

Due to the low number of experimental levels and relatively high number of parameters, the refinement of all parameters had to be carried out with utmost care. For example, the starting values for the free ion parameters those of the TbOCl [20] system were used. The initial c.f. parameter values were taken from earlier calculations for the same system. The final set of the free ion (Table 2) and c.f. parameters was obtained by a least-squares fitting procedure between the experimental and calculated energy level values by minimizing the mean square deviation between the energy level values using the matrix diagonalization and least squares refinement program package REEL [31].

The energy level scheme of the $\mathrm{Gd}^{3+}$ ion was simulated well (Table 1). Despite to low degrees of freedom, a good agreement between the observed and calculated level values was achieved but the rms deviation remained rather high, 21 $\mathrm{cm}^{-1}$. The estimated standard deviations of the parameter values are obviously very large, too. The calculated splitting of the $^8S_{7/2}$ ground level is minute — less than 2 $\mathrm{cm}^{-1}$ and can thus not be observed in the absorption spectra. The weak splitting of the $^8S_{7/2}$ level is in good agreement with the ESR measurements carried out in other $\mathrm{Gd}^{3+}$ doped systems [32].

The c.f. parameter set obtained here for GdOCl ($B_0^2 - 950(110)$; $B_0^4 - 600(440)$; $B_4^4 \pm 850(250)$; $B_0^6 980(330)$ and $B_4^6 \pm 200(1050)$) is in agreement with the parameters for other REOCl (or GdOCl:$\mathrm{RE}^{3+}$) ($\mathrm{RE}^{3+} = \mathrm{Pr}^{3+}$ [17], $\mathrm{Nd}^{3+}$ [18], $\mathrm{Sm}^{3+}$, $\mathrm{Eu}^{3+}$ [19], $\mathrm{Tb}^{3+}$ [20], $\mathrm{Dy}^{3+}$ [21], $\mathrm{Ho}^{3+}$ [22], $\mathrm{Er}^{3+}$ [23], and $\mathrm{Tm}^{3+}$ [24]) studied so far. The use of the ± sign is due to the impossibility to distinguish between certain energy levels. There is a smooth increase in the $F^K$ and $\zeta_{4\mathrm{f}}$ free ion parameters from $\mathrm{Pr}^{3+}$ to $\mathrm{Tm}^{3+}$ (Table 2) indicating increasing electrostatic repulsion and spin–orbit coupling between the 4f electrons.

Table 2
Evolution of the free ion parameter values in the REOCl series (in $cm^{-1}$)

| $RE^{3+}$ | $F^2$ | $F^4$ | $F^6$ | $\alpha$ | $\beta$ | $\gamma$ | $\zeta_{4f}$ |
|---|---|---|---|---|---|---|---|
| $Pr^{3+}$ | 67 659(30) | 49 458(45) | 32 813(7) | 23.6(1) | −676(2) | 1422 | 742(1) |
| $Nd^{3+}$ | 70 488(105) | 50 945(90) | 35 068(110) | 19.6(3) | −647(12) | 1791(30) | 870(2) |
| $Sm^{3+}$ | 78 167(5) | 55 878(22) | 39 779(5) | 19.7(0.2) | −590(2) | 1654(2) | 1150(1) |
| $Gd^{3+}$ | 87 086(6) | 58 080(13) | 45 360(10) | 19.1(1) | −742(3) | 1654(2) | 1556(3) |
| $Tb^{3+}$ | 89 471(15) | 63 055(22) | 44 081(8) | 19.6(0.3) | −769(2) | 1823(6) | 1686(1) |
| $Dy^{3+}$ | 91 990(5) | 64 704(22) | 46 170(4) | 19.2(0.2) | −750(2) | 1860(2) | 1900(1) |
| $Ho^{3+}$ | 95 105(15) | 67 548(22) | 47 518(8) | 18.9(0.2) | −665(2) | 1907(3) | 2129(1) |
| $Er^{3+}$ | 98 479(15) | 69 888(43) | 51 115(8) | 18.7(0.4) | −768(4) | 1751(7) | 2381(1) |
| $Tm^{3+}$ | 100 759(60) | 70 735(63) | 51 904(24) | 19.2(0.9) | −877(12) | 1845(23) | 2616(1) |

## 4. Conclusions

A total of 24 c.f. components representing seven $^{2S+1}L_J$ levels of the $Gd^{3+}$ ion were resolved from the analyses of the absorption spectra of GdOCl. Despite the low number of the experimental data and the high degeneracy of the $4f^7$ electron configuration, the energy level scheme of the $Gd^{3+}$ ion in GdOCl was successfully simulated according to the $C_{4v}$ site symmetry by a phenomenological model using 14 free ion and five c.f. parameters yielding a rms deviation of 21 $cm^{-1}$. The results for GdOCl are consistent with those for other $RE^{3+}$ ($Pr^{3+}$, $Nd^{3+}$, $Sm^{3+}$, $Eu^{3+}$, $Tb^{3+}$, $Dy^{3+}$, $Ho^{3+}$, $Er^{3+}$, and $Tm^{3+}$) in the REOCl hosts.

## References

[1] R.T. Wegh, H. Donker, A. Meijerink, R.-J. Lamminmäki, J. Hölsä, Phys. Rev. B 56 (1997) 13841.
[2] R.T. Wegh, E.V.D. van Loef, A. Meijerink, J. Luminesc. 90 (2000) 111.
[3] R.T. Wegh, H. Donker, E.V.D. van Loef, K.D. Oskam, A. Meijerink, J. Luminesc. 87–89 (2000) 1017.
[4] K.D. Oskam, R.T. Wegh, H. Donker, E.V.D. van Loef, A. Meijerink, J. Alloys Comp. 300–301 (2000) 421.
[5] G.H. Dieke, in: Spectra and Energy Levels of Rare Earth Ions in Crystals, Wiley Interscience, New York, 1968.
[6] R.H.T. Wegh, A. Meijerink, R.-J. Lamminmäki, J. Hölsä, J. Luminesc. 87–89 (2000) 1002.
[7] P. Porcher, Phase Trans. 13 (1988) 233.
[8] W.T. Carnall, G.L. Goodman, K. Rajnak, R.S. Rana, J. Chem. Phys. 90 (1989) 3443.
[9] J. Makovsky, Phys. Lett. 19 (1966) 647.
[10] C.K. Jayasankar, F.S. Richardson, J. Less-Common Met. 148 (1989) 289.
[11] P.A. Tanner, V.V. Ravi Kanth Kumar, C.K. Jayasankar, M.F. Reid, J. Alloys Comp. 215 (1994) 349.
[12] R.L. Schwiesow, H.M. Crosswhite, J. Opt. Soc. Am. 59 (1969) 592.
[13] C.A. Morrison, R.P. Leavitt, in: K.A. Gschneidner Jr., L. Eyring (Eds.), Handbook of the Physics and Chemistry of Rare Earths, North Holland, Amsterdam, 1982, p. 461.
[14] K.A. Schoene, J.R. Quagliano, F.S. Richardson, Inorg. Chem. 30 (1991) 3803.
[15] P. Dorenbos, J. Luminesc. 87–89 (2000) 970.
[16] P. Dorenbos, J. Luminesc. 91 (2000) 91.
[17] E. Antic-Fidancev, J. Hölsä, M. Lemaître-Blaise, P. Porcher, J. Chem. Soc.: Faraday Trans. 87 (1991) 3625.
[18] Beaury, L., Ph.D. Thesis, Université de Paris-Sud, Orsay France, 1988.
[19] J. Hölsä, P. Porcher, J. Chem. Phys. 75 (1981) 2108.
[20] J. Hölsä, R.-J. Lamminmäki, P. Porcher, H.F. Brito, Quim. Nova 19 (1996) 237.
[21] J. Hölsä, R.-J. Lamminmäki, P. Porcher, P. Dereń, W. Stręk, Spectrochim. Acta A54 (1998) 2189.
[22] J. Hölsä, R.-J. Lamminmäki, M. Lastusaari, E.P. Chukalina, M.N. Popova, P. Porcher, J. Luminesc. 87–89 (2000) 1052.
[23] J. Hölsä, E. Säilynoja, R.-J. Lamminmäki, P. Dereń, W. Stręk, P. Porcher, J. Chem. Soc.: Faraday Trans. 93 (1997) 2241.
[24] J. Hölsä, R.-J. Lamminmäki, E. Antic-Fidancev, M. Lemaître-Blaise, P. Porcher, J. Phys.: Condens. Matter 7 (1995) 5127.
[25] J. Hölsä, L. Niinistö, Thermochim. Acta 37 (1980) 155.
[26] D.H. Templeton, C.H. Dauben, J. Am. Chem. Soc. 75 (1953) 6069.
[27] P. Caro, J. Less-Common Met. 16 (1968) 367.
[28] J.L. Prather, NBS Monograph (US) 19 (1961) 42.
[29] B.G. Wybourne, in: Spectroscopic Properties of Rare Earths, Interscience, New York, 1965, Chapter 6.
[30] H. Crosswhite, H.M. Crosswhite, B.R. Judd, Phys. Rev. 169 (1979) 11.
[31] Porcher, P., Computer Program REEL for the Simulation of $d^N$ and $f^N$ Configurations Involving the Real and Complex Crystal Field Parameters, CNRS, Meudon France, 1989 (unpublished).
[32] K.J. Guedes, K. Krambrock, J.Y. Gesland, J. Phys: Condens. Matter 11 (1999) 7211.